NUWC-NPT Technical Document 11,037
28 August 1995

12

A Compilation of Geometric Distance and Tissue Property Data for the Human Thorax

Cathy A. Norton
Submarine Sonar Department

Naval Undersea Warfare Center Division
Newport, Rhode Island

PREFACE

The work described in this document was sponsored by the Office of Naval Research (ONR) Fellowship Program. The author, who is a doctoral candidate at the University of California, Berkeley, conducted this research while at the Naval Undersea Warfare Center (NUWC) Detachment New London during the summer of 1995. The investigation supports a modeling effort of the NUWC Division Newport Independent Research (IR) Program under Project B10004, *Detection and Localization of Internal Acoustic Emissions in a Three-Dimensional Structure*, principal investigator Dr. A. J. Hull (Code 2141). The IR program is funded by ONR; the NUWC Division Newport program manager is Dr. S. C. Dickinson (Code 102).

This investigation was also conducted in conjunction with the Medacoustics Corporation through the CRADA program (NCRADA-94-006), *Noninvasive Detection and Location of Coronary Artery Disease*, under Project N68021, principal investigator Dr. N. L. Owsley (Code 2123).

The author wishes to thank Karen Holt (Code 0251) of NUWC Detachment New London for her help with the technical editing.

Reviewed and Approved: 28 August 1995

R. J. Martin
Acting Head, Submarine Sonar Department

REPORT DOCUMENTATION PAGE

Form Approved
OMB No. 0704-0188

1. AGENCY USE ONLY (Leave Blank)	2. REPORT DATE	3. REPORT TYPE AND DATES COVERED
	28 August 1995	Final

4. TITLE AND SUBTITLE

A Compilation of Geometric Distance and Tissue Property Data for the Human Thorax

5. FUNDING NUMBERS

6. AUTHOR(S)

Cathy A. Norton

7. PERFORMING ORGANIZATION NAME(S) AND ADDRESS(ES)

Naval Undersea Warfare Center
Detachment New London
New London, Connecticut 06320

8. PERFORMING ORGANIZATION REPORT NUMBER

TD 11,037

9. SPONSORING/MONITORING AGENCY NAME(S) AND ADDRESS(ES)

Office of Naval Research
800 North Quincy Street
Arlington, VA 22217-5000

10. SPONSORING/MONITORING AGENCY REPORT NUMBER

11. SUPPLEMENTARY NOTES

The author of this document, a doctoral candidate at the University of California, Berkeley, was a participant in the ONR Fellowship Program at NUWC Detachment New London during the summer of 1995.

12a. DISTRIBUTION/AVAILABILITY STATEMENT

Approved for public release; distribution is unlimited.

12b. DISTRIBUTION CODE

13. ABSTRACT (Maximum 200 words)

This document is a collection of information from the scientific literature that is relevant to the modeling of sound transmission in the human thorax. It contains data on geometric distances from points on the chest wall to the sites of sound generation within the heart and coronary arteries. The spectral content of the sound is also discussed. The types and thicknesses of tissues along the direct path for sound transmission are identified, and a description of the viscoelastic tissue properties of the thorax is provided.

14. SUBJECT TERMS

Coronary Artery Disease, Human Thorax, Noninvasive Passive Detection, Space-Time Vibrational Field, Thorax Geometry, Thorax Tissue, Vibroacoustic Sensor

15. NUMBER OF PAGES
28

16. PRICE CODE

17. SECURITY CLASSIFICATION OF REPORT	18. SECURITY CLASSIFICATION OF THIS PAGE	19. SECURITY CLASSIFICATION OF ABSTRACT	20. LIMITATION OF ABSTRACT
UNCLASSIFIED	UNCLASSIFIED	UNCLASSIFIED	SAR

TABLE OF CONTENTS

LIST OF ILLUSTRATIONS

LIST OF TABLES

LIST OF MEDICAL NOMENCLATURE

C	Left Circumflex Coronary Artery
CA	Coronary Artery
CAD	Coronary Artery Disease
CD	Posterior Descending Artery of Left Circumflex Artery
CI	Inferior Wall Branch of Left Circumflex Artery
CP	Posterior Wall Branch of Left Circumflex Artery
D	Diagonal Branch of Left Anterior Coronary Artery
L	Left Anterior Descending Coronary Artery
LCA	Left Coronary Artery
LM	Left Main Coronary Artery
M	Marginal Branch of Left Circumflex Artery
MR	Median Ramus
OM	Obtuse Marginal Branch of Left Circumflex Artery
RCA	Right Coronary Artery
RD	Descending Branch of Right Coronary Artery
RI	Inferior Wall Branch of Right Coronary Artery
RP	Posterior Wall Branch of Right Coronary Artery
S	Septal Perforator
S1	First Heart Sound
S2	Second Heart Sound
S3	Third Heart Sound
S4	Fourth Heart Sound

A COMPILATION OF GEOMETRIC DISTANCE AND TISSUE PROPERTY DATA FOR THE HUMAN THORAX

INTRODUCTION

This document summarizes the anatomical and physiological data from the literature that is needed in the development of a noninvasive passive detection method for coronary artery disease. It has been proposed to measure the space-time vibrational field of the chest wall caused by coronary artery occlusions with an array of vibroacoustic sensors.[1] Turbulence-induced wall stresses in the artery result in wave energy transfer to the body surface. This low-level acoustic energy can be distinguished from other physiological sounds by its temporal, spectral, and spatial characteristics. However, it is first necessary to identify the various noise sources within the thorax and the spectral content of the signals they produce. It is also important to know the location of the noise-producing elements, such as the heart valves and any occluded coronary arteries, and the timing of their sounds within the heart cycle.

The following sections describe the spectral and temporal characteristics of various physiological sounds. Thorax geometry and tissue properties are also discussed.

CARDIOPULMONARY SOUNDS

The four basic heart sounds are described in this section, and the generally accepted theories of their origins are presented. Figure 1 shows the relationship between the heart sounds and various cardiac events.

The most prominent heart sounds are the first and second sounds, known as S1 and S2. These two sounds are easily identified because they occur during systole. Additionally, the main frequency components lie below 150 for S1 (reference 2) and below 170 Hz for S2, with the peak frequencies of S2 around 50-70 Hz.[3,4] The sound S1 has two components corresponding to the closing of the mitral and tricuspid valves. Similarly, S2 has two components but they are related to the closing of the aortic and pulmonary valves.

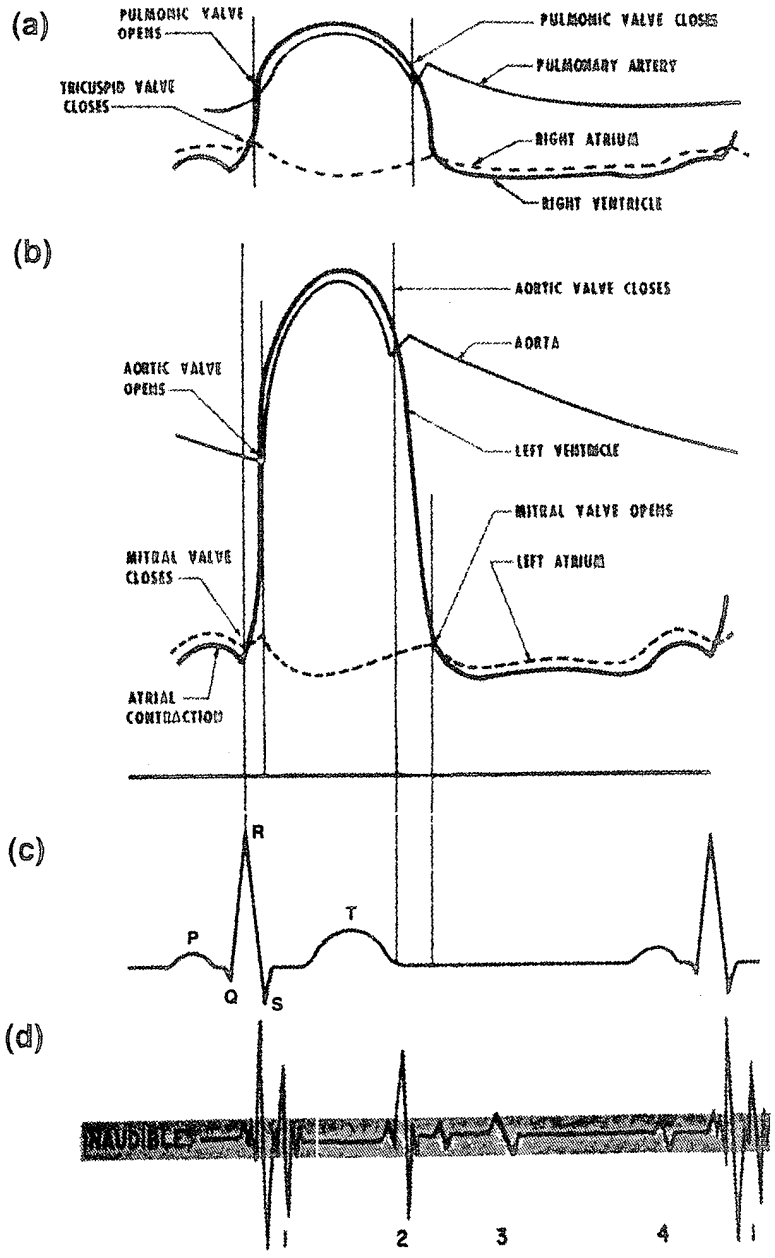

Figure 1. Heart Sounds and Cardiac Events: (a) Pressure in Right Heart, (b) Pressure in Left Heart, (c) Electrocardiogram, and (d) Heart Sounds

The third heart sound, S3, occurs during diastole approximately 0.13-0.18 seconds after S2. It is associated with the rapid deceleration of blood and a sharp pressure rise in the ventricles. This is most likely the turbulence due to deceleration of the mitral jet. S3 is audible in most children, but is generally believed to lessen in intensity with age. A recent study, however, found an audible S3 in 23 percent of a population of healthy 37-year olds, a higher incidence than expected.[5] This third heart sound has also been correlated with the presence of left ventricular failure, including that caused by coronary artery disease (CAD). Although there is a statistically significant relationship between an audible S3 and a change in myocardial viscoelasticity, disagreement exists over whether increased compliance[6] or stiffness[7] is associated with the onset of S3. No spectral data were found in the literature.

The fourth heart sound (S4) is a low-frequency noise (40-60 Hz)[8] heard near end diastole, just prior to S1. Its occurrence coincides with the abrupt increase in both ventricular volume and pressure caused by atrial contraction. It is common in CAD patients, especially during ischemic periods and following myocardial infarction. A "summation sound" - an overlap of S3 and S4- may occur in ventricular failure when atrial contraction occurs simultaneously with the rapid filling phase.

Based on the prevalence of audible S3 in a healthy adult population and the increased likelihood of S3 and S4 in patients with CAD, it is probable that there will be some diastolic flow noise (sometimes called diastolic murmur) associated with transmitral flow, although it will not necessarily be audible.

The sounds that are of interest (those produced in stenosed coronary arteries) occur during diastole. Their measured spectral content is highly dependent on the processing method that is used.[9] However, all clinical and theoretical values fall within the 200-800 Hz range as shown in table 1.[9-11]

Based on the above information it is possible to distinguish between the vibrations due to turbulence in stenosed arteries and those due to the S1, S2, and S4 sounds. The signal can be temporally filtered and only the diastolic portion analyzed. This eliminates the high intensity S1 and S2 signals. Furthermore, S4 has a much lower frequency range than signals arising from CAD and can therefore be distinguished on the basis of spectral content.

Noise generated in the lungs during inspiration and expiration must be considered as another sound source. Ploysongsang et al. investigated inspiratory and expiratory vesicular breath sounds and found that most energy is contained below 200 Hz, with a peak occurring between 35 and 55 Hz.[12] The inspiratory sound is heard throughout inspiration while the quieter expiratory sound lasts for only the first third of expiration. Although the breathing sounds overlap the low end of the frequency range associated with CAD diastolic murmurs, they are easily eliminated by having the patient "hold his breath" during the course of measurements.

Table 1. Summary of Cardiopulmonary Sounds

Sound	Frequency Range (Hz)	Peak Frequency (Hz)	Probable Source	Time of Occurrence
S1	0-150	--	mitral and tricuspid closure	systole
S2	0-170	30-70	aortic and pulmonary closure	systole
S3	--	--	rapid filling of ventricles	diastole: 0.13-0.18 sec after S2
S4	20-60	--	atrial contraction	diastole: 0.08-0.10 sec after beginning of P wave
Stenosis	200-800	--		diastole
Breathing	0-200	36-41 36-57		inspiration 1/3 expiration

GEOMETRIC DATA

The Euclidean distances from the heart valves (the major noise sources) and clinically or anatomically significant points along the main coronary arteries to three points on the chest wall were determined. Figures 2 and 3 show the locations of two such points, P1 and P2, on the chest. The distance to the middle of the sternum at the third costal cartilage was also established as a reference. The two chest wall positions were chosen as potential sites for sensor location during chest wall vibration measurements on human subjects. The first measurement point (P1) is located in the third intercostal space, 4 centimeters from the midline of the sternum. The second measurement point (P2) is located in the space just medial to the seventh costal cartilage, 6.25 centimeters from the midline. This P2 position allows measurement of the chest wall vibrations without interference from the ribs.

LOCATION OF HEART VALVES

Figure 2 shows the location of the heart relative to the ribs and vertebrae.[13] The heart extends from the fifth to tenth thoracic vertebra in this adult male of unknown age. The aortic valve is located at the level of the upper portion of the seventh thoracic vertebra (T7), and the mitral valve is located at the center of the eighth thoracic vertebra. The pulmonary valve is located at the level of the lower third of the sixth thoracic vertebra, and the tricuspid valve is directly behind the sternum at the eighth vertebral disk. Table 2 shows the average position of the heart valves, base (top), and apex (bottom) with respect to vertebral level for 11 adult males.[13]

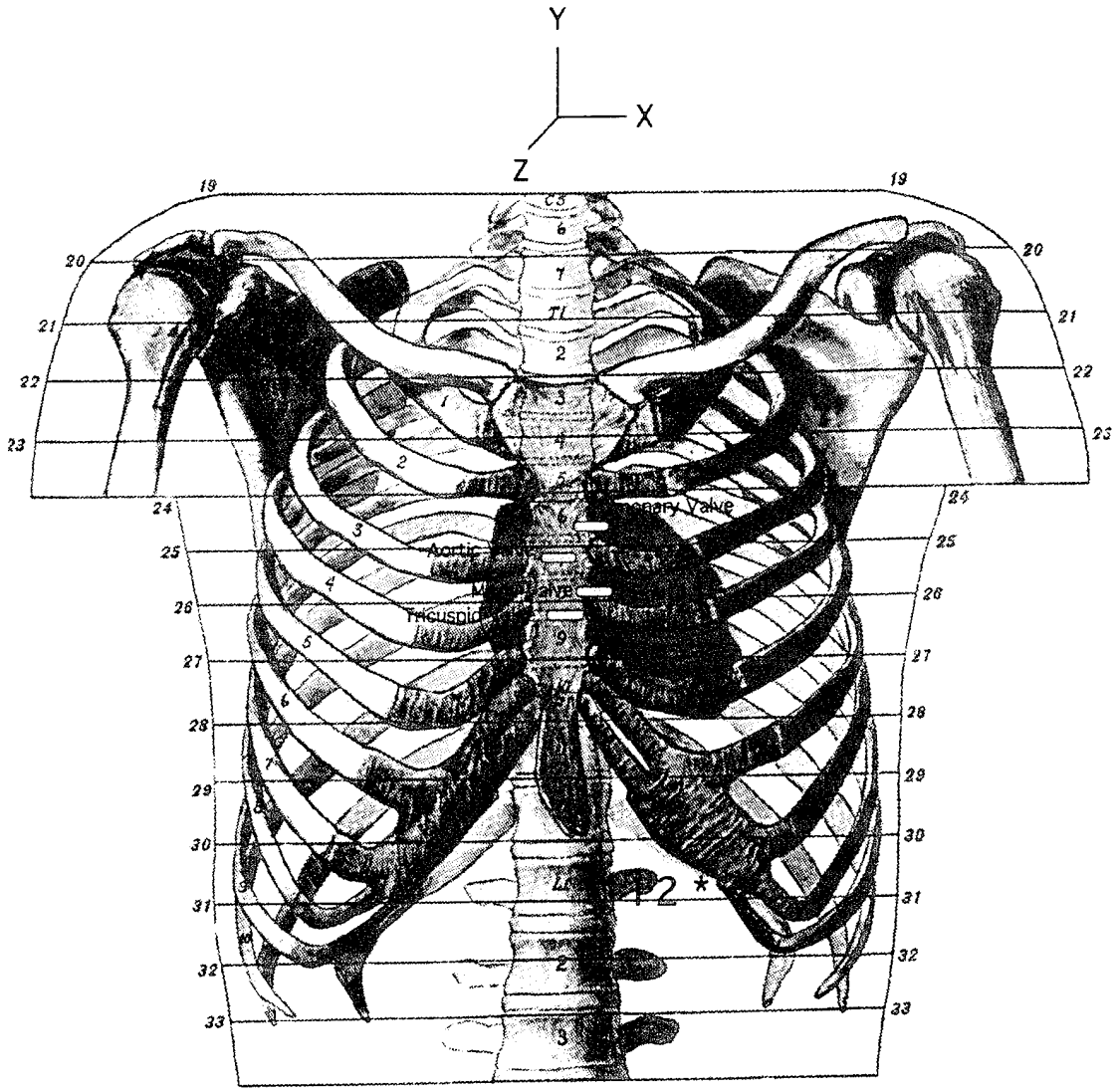

Figure 2. Heart Position Relative to Skeletal Structure

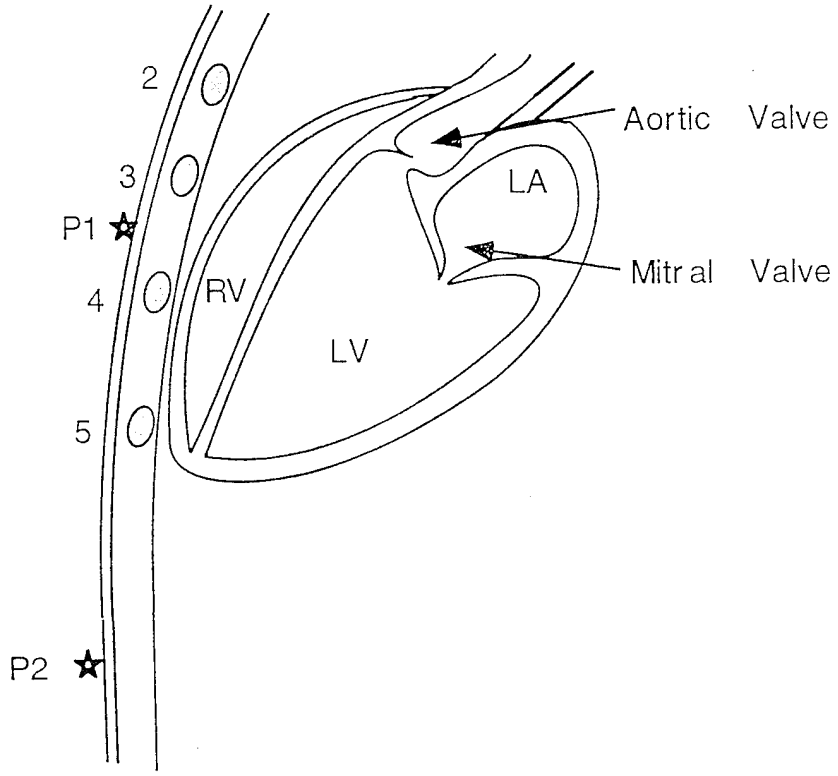

Figure 3. Side View of Chest Showing Position and Orientation of Heart

Table 2. Position of Heart Referenced to Vertebrae

	Average Position	Range
Base	(m,l) T3	(l) T4 - (u) T8
Apex	(l) T10	D8 - D11
Aortic Valve	(m) T7	D5 - (u) T9
Mitral Valve	(m) T8	(m) T6 - (u)T10
Pulmonary Valve	D6	D4 - (l) T8
Tricuspid Valve	(u) T9	(u) T7 - (m) T10

Notation: T- thoracic vertebra.

(u,m,l) - indicates the upper, middle, or lower third of the vertebra.

D- vertebral disk, with the number corresponding to the vertebra directly above it.

Figure 3 shows a cross section of the heart in a side view. The mitral valve plane forms an angle of approximately 30 degrees with the horizontal, directing the mitral jet inferiorly and anteriorly toward the apex of the heart and the fifth intercostal space. This apical position is in fact the classic auscultation point for listening to the S1 and S3 sounds associated with the mitral valve.[8]

Measurements of the geometric position of the heart valves and coronary artery ostia within the thorax were based on the cross sectional anatomy. A coordinate axis was defined with the origin on the chest wall as indicated in figure 2. The left lateral direction is the x-coordinate, the vertical (cephalid) direction is the y-coordinate, and the anterior direction is the z-coordinate. Table 3 shows the coordinates and depth of the valves measured from the two chest wall locations.

Although no information is provided regarding the time within the cardiac cycle for the subject of the cross-sectional study, the position of the heart valves is consistent with diastole.

Table 3. Location of Heart Valves Referenced to Chest Wall

	Distance from P1				Distance from P2			
	z1	x1	y1	r1	z2	x2	y2	r2
Aortic valve	-7.63	-3.50	1.38	8.50	-9.38	-5.75	14.00	17.80
Mitral valve	-8.56	-1.50	-0.13	8.69	-10.31	-3.75	12.50	16.63
Tricuspid valve	-5.50	-4.00	-1.00	6.87	-7.25	-6.25	11.63	15.06
Pulmonary valve	-7.44	-3.00	2.63	8.44	-9.19	-5.25	15.25	18.56

LOCATION OF CORONARY ARTERIES

Data for the coronary arteries was adapted from Dodge et al.[14] They determined the interthoracic location of 23 coronary artery (CA) segments at end diastole from the angiographic data of 37 patients. The CA anatomy of each patient can be categorized based on the origin of the arteries that supply the inferior ventricular septum. The patient is right coronary artery (RCA) dominant if the branches arise from the right coronary artery, left coronary artery (LCA) dominant if they arise from the left anterior descending artery, or balanced if both vessels supply the inferior wall. Most patients in this study (30/37) were classified as RCA dominant. A description of the three main coronary arteries, including important branches, follows next. Figure 4 illustrates the CA structure and nomenclature used for segment identification.

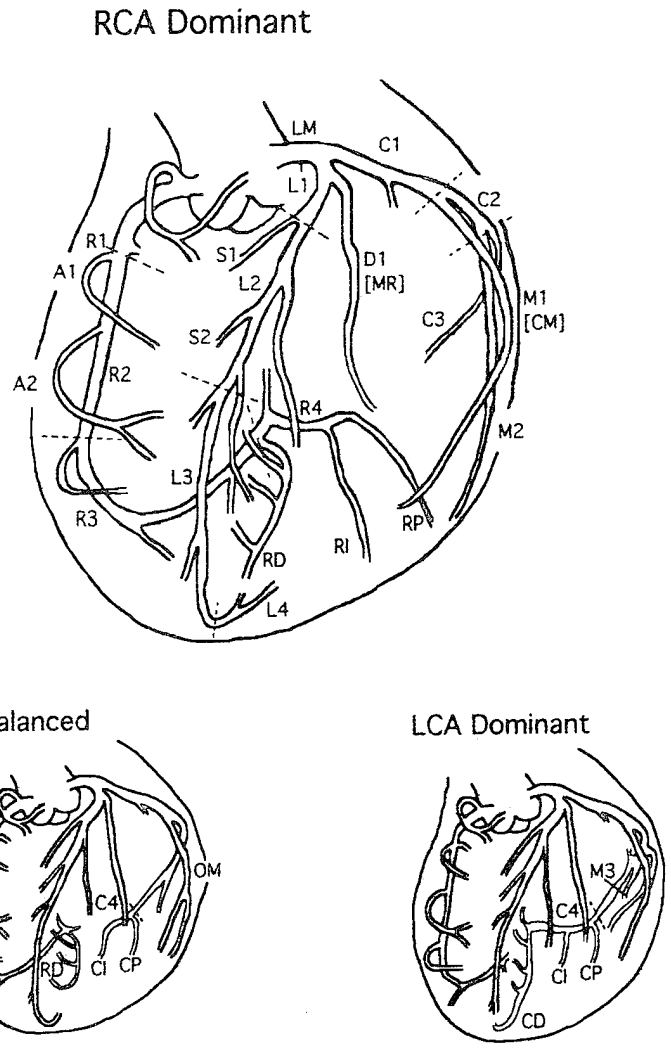

Figure 4. Coronary Artery Structure

The right main coronary artery (RCA) arises from the right coronary ostia. The midpoints of four segments (R1- R4) of the main branch were determined. The midpoints of the posterior descending branch (RD), posterior wall branch (RP), and inferior wall branch (RI) are also given. In the balanced anatomy, only the posterior descending branch is identified. In an LCA-dominant heart, no inferior wall vessels arise from the RCA.

The left main coronary artery (LM) originates at the left coronary ostia and bifurcates into the left anterior descending (L) and left circumflex (C) arteries. The left anterior descending artery is divided into four segments. The midpoints of each of the segments is identified, as well as the proximal points of segments L1 and L4 (apex). The main branches of the left anterior descending coronary artery include three septal perforators (S1-S3) and diagonal branches (D1-D3). In the case where the LM trifurcates, the middle branch is identified as the median ramus (MR). The left circumflex artery has been divided into segments C1-C3, with marginal branches M1 and M2. A large obtuse marginal branch (OM) in some cases replaces the two marginal branches. In the balanced anatomy, a fourth segment of the circumflex artery is present with posterior and inferior wall branches (CP and CI). There is an additional branch in LCA-dominant anatomies: the posterior descending coronary artery (CD).

The cross-sectional anatomy of figure 2 was also used to locate the coronary ostia relative to the reference position on the chest wall. The arterial data was then transformed into the orthogonal coordinate system defined above. The locations of the left anterior descending CA segments with respect to measurement locations P1 and P2 are presented in table 4, the left circumflex artery in table 5, and the right coronary artery in table 6.

Table 4. Left Anterior Descending Coronary Artery Segment Locations

	Distance from P1				Distance from P2			
	z1	x1	y1	r1	z2	x2	y2	r2
LM mid	-9.47	-1.87	3.37	10.22	-2.97	-4.12	15.99	16.78
L1 prox	-9.04	-1.06	3.24	9.66	-2.54	-3.31	15.86	16.40
L1 mid	-8.55	-0.52	3.12	9.11	-2.05	-2.77	15.75	16.12
L2 mid	-5.86	1.04	2.22	6.35	0.64	-1.21	14.84	14.91
L3 mid	-2.17	1.72	-2.03	3.43	4.33	-0.53	10.59	11.46
L4 prox	-2.40	1.93	-5.46	6.26	4.10	-0.32	7.17	8.27
L4 mid	-3.09	1.66	-5.58	6.60	3.41	-0.59	7.04	7.84
D1 orig	-8.05	0.21	2.88	8.55	-1.55	-2.04	15.50	15.71
D1 mid	-6.82	2.43	0.90	7.30	-0.32	0.18	13.52	13.53
D2 orig	-6.32	0.94	2.30	6.79	0.18	-1.31	14.93	14.99
D2 mid	-4.97	2.75	0.19	5.68	1.53	0.50	12.81	12.91
D3 orig	-4.82	1.58	1.39	5.26	1.68	-0.67	14.02	14.13
D3 mid	-3.58	2.85	-0.62	4.62	2.92	0.60	12.00	12.37
S1 orig	-7.81	0.17	2.80	8.30	-1.31	-2.08	15.43	15.62
S1 mid	-6.57	-0.45	1.11	6.67	-0.07	-2.70	13.73	13.99
S2 orig	-5.93	0.97	2.24	6.41	0.57	-1.28	14.86	14.93
S2 mid	-5.24	0.05	0.51	5.26	1.26	-2.20	13.13	13.38
S3 orig	-4.30	1.42	1.04	4.65	2.20	-0.83	13.67	13.87
S3 mid	-4.17	0.57	-0.44	4.23	2.33	-1.68	12.19	12.52

Table 5. Left Circumflex Artery Segment Locations

	Distance from P1				Distance from P2			
	z1	x1	y1	r1	z2	x2	y2	r2
C1 prox	-9.49	-1.19	3.03	10.03	-2.99	-3.44	15.65	16.31
C1 mid	-9.70	-0.92	2.59	10.08	-3.20	-3.17	15.21	15.87
C2 mid	-10.67	-0.34	1.46	10.78	-4.17	-2.59	14.08	14.91
C3 mid	-11.72	-0.42	-0.41	11.74	-5.22	-2.67	12.22	13.55
C4 mid	-11.45	-2.10	-2.26	11.86	-4.95	-4.35	10.37	12.28
MR orig	-9.48	-1.38	3.11	10.08	-2.98	-3.63	15.74	16.42
MR mid	-8.78	2.01	0.19	9.01	-2.28	-0.24	12.81	13.02
OM orig	-10.12	-0.42	2.15	10.35	-3.62	-2.67	14.77	15.44
OM bifur	-10.61	0.80	0.67	10.67	-4.11	-1.45	13.30	13.99
OM ant mid	-10.39	1.23	-0.29	10.47	-3.89	-1.02	12.33	12.97
OM pos mid	-11.04	0.71	-0.02	11.07	-4.54	-1.54	12.60	13.49
M1 orig	-9.98	-0.72	2.19	10.24	-3.48	-2.97	14.81	15.50
M1 mid	-9.66	1.85	-0.13	9.84	-3.16	-0.40	12.50	12.90
M2 orig	-10.79	-0.29	1.09	10.85	-4.29	-2.54	13.72	14.59
M2 mid	-10.82	1.01	-1.34	10.95	-4.32	-1.24	11.28	12.14
M3 orig	-11.61	-0.23	-0.23	11.61	-5.11	-2.48	12.40	13.64
M3 mid	-11.20	0.48	-2.19	11.43	-4.70	-1.77	10.43	11.58

Table 6. Right Coronary Artery Segment Locations

	Distance from P1				Distance from P2			
	z1	x1	y1	r1	z2	x2	y2	r2
R1 prox	-6.35	-4.44	1.69	7.93	0.15	-6.69	14.31	15.80
R1 mid	-5.92	-5.44	1.18	8.13	0.58	-7.69	13.81	15.82
R2 mid	-5.55	-6.93	-1.54	9.01	0.95	-9.18	11.08	14.42
R3 mid	-6.54	-6.29	-4.10	9.96	-0.04	-8.54	8.53	12.07
R4 mid	-9.02	-4.00	-3.79	10.57	-2.52	-6.25	8.84	11.11
RD mid	-6.18	-2.19	-5.50	8.56	0.32	-4.44	7.13	8.40
RI mid	-8.77	-2.29	-5.17	10.44	-2.27	-4.54	7.45	9.02
RP mid	-10.16	-1.43	-4.76	11.31	-3.66	-3.68	7.87	9.43

IDENTIFICATION OF TISSUE LAYERS

The types and thicknesses of tissues along the paths from sensor location P1 on the chest wall to the heart valves were estimated, with results presented in table 7. The intervening tissues between P1 and the four valves were identified on all cross sections from levels 24 through 27.[13] Measurements were interpolated for vertical positions between displayed cross-sectional layers. It is important to note that the reported dimensions are for a particular human subject and that no attempt was made to determine the variation in such measurements across a larger sample population. Verburg et al.[4] assume that the properties of lung tissue will dominate the sound transmission from the heart to the chest wall. However, most of the literature shows that for locations close to the sternum (such as P1) the direct transmission paths of the mitral, aortic, and tricuspid valves do not pass through any lung tissue because of the cardiac notch in the left lobe of the lungs. Therefore, lung properties will have little influence on the direct path sound transmission characteristics of the thorax.

Table 7. Tissue Thickness (cm) Between P1 and Cardiac Valves

	Aortic	Mitral	Pulmonary	Tricuspid
Dermis	0.25	0.25	0.25	0.25
Adipose tissue	0.51	0.50	0.50	0.63
Muscle	1.58	1.00	1.30	1.45
C.m.a.	0.51	0.75	0.60	0.82
C.p.	0.38	-	0.40	-
Lung	-	-	0.80	-
Pericardium	0.13	0.15	0.15	0.19
Interior heart	5.14	6.04	4.44	3.53

C.m.a. = Cavum mediastinale anterius

C.p. = Cavum pleurae

The direct paths from the valves to P2 will pass through successive layers of the heart, pericardium, diaphragm, liver, abdominal muscle, subcutaneous fat, and skin. Estimation of tissue thicknesses was not made because of an inadequate resolution of the cross-sectional anatomy and the lack of tissue property data (discussed next).

TISSUE PROPERTIES

Yen and Fung[15] estimate a wave speed in the chest wall of 1000 m/s. Verburg reports values on the order of 1500 m/s for compressional waves and 10 m/s for shear waves at 1000 Hz. The soft tissue and composite (lung and soft tissue) viscoelastic properties of Verburg presented in table 8 were used to calculate the shear wave speeds in table 9.

Table 8. Viscoelastic Tissue Properties

	Lung	Soft Tissue	Composite
ρ (kg/m^3)	250	1100	300
G (μ_1) (N/m^2)	300	5000	300
μ_2 (Ns/m^2)	300	50	50
ν (Poisson's ratio)	0.5	--	--
λ_1 (N/m^2)	--	2.6 E+9	1.25 E+8
λ_2	0.0	0.0	0.0

Table 9. Shear Wave Speeds in Chest Wall

Frequency (Hz)	Soft tissue wave speed (m/s)	Composite tissue wave speed (m/s)
1	2.13	1.01
10	2.14	1.60
100	2.74	5.61
500	6.22	12.83
1000	9.11	18.20

Durand[3] calculated the sound transmission properties in the ascending aorta of dogs. The phase of the transfer function between two micromanometers placed in the aorta was used to estimate the phase velocity of sound waves through blood in the ascending

aorta. Between 40 and 100 Hz, the phase speed was constant at 5.5 m/s. It reached a peak of 9 m/s at 300 Hz and then decreased to a steady value of 8 m/s beyond 500 Hz. These wave speeds are much lower than the speed of compressional waves in blood (~ 1500 m/s) because the effective stiffness of the fluid and vessel is limited by the lower value-- in this case the aorta stiffness.[3]

No further discrimination among tissue types was found in the literature. Therefore, development of a model for sound transmission will likely assume homogeneous tissue properties within the thorax.

REFERENCES

1. N. L. Owsley, M. H. Ahmed, A. J. Hull, and J. Kassal, "Space-Time Characteristics of the Turbulent Flow Energy in a Viscoelastic Medium Using Noninvasive Passive Imaging," NUWC-NPT Technical Report 10,833, Naval Undersea Warfare Center Detachment, New London, Connecticut, 8 March 1995.

2. J. C. Wood, A. Buda, and D. T. Barry, "Time-Frequency Transforms: A New Approach to First Heart Sound Frequency Dynamics," *IEEE Transactions on Biomedical Engineering*, vol. 39, no. 7, July 1992, pp. 730-740.

3. L.-G. Durand, Y. E. Langlois, T. Lanthier, R. Chiarella, P. Coppens, S. Carioto, and S. Bertrand-Bradley, "Acoustic Transmission of the Aortic Component of the Second Heart Sound Within the Ascending Aorta of Dogs," *Medical and Biological Engineering and Computing,* vol. 29, 1991, pp. 281-286.

4. J. Verburg., "Transmission of Vibrations of the Heart to the Chestwall," *Advanced Cardiovasclar Physiology,* vol. 5, part III, 1983, pp. 84-103.

5. M. Kupari, P. Koskinen, J. Virolainen, P. Hekali, and P. Keto, "Prevalence and Predictors of Audible Physiological Third Heart Sound in a Population Sample Aged 36 to 37 Years," *Circulation*, vol. 89, no. 3, March 1994, pp. 1189-1195.

6. G. M. Drzewiecki, M. J. Wasicko, and J. K-J. Li, "Diastolic Mechanics and the Origin of the Third Heart Sound," *Annals of Biomedical Engineering*, vol. 19, 1991, pp. 651-667.

7. K. Tatsuji, H. Rosman, M. Alam, P. D. Stein, and H. Sabbah, "Hemodynamic Correlates of the Third Heart Sound During the Evolution of Chronic Heart Failure," *Journal of the American College of Cardiology*, vol. 21, no. 2, February 1993, pp. 419-423.

8. A. Ravin, L. D. Craddock, P. S. Wolf, and D. Shander, *Auscultation of the Heart*, 3rd ed., Year Book Medical Publishers, Chicago, 1977.

9. Y. M. Akay, M. Akay, W. Welkowitz, J. L. Semmlow, and J. B. Kostis, "Noninvasive Acoustical Detection of Coronary Artery Disease: A Comparative Study of Signal Processing Methods," *IEEE Transactions on Biomedical Engineering*, vol. 40, no. 6, June 1993, pp. 571-578.

10. M. Akay, W. Welkowitz, J. L. Semmlow, and J. Kostis, "Application of the ARMA Method to Acoustic Detection of Coronary Artery Disease," *Medical and Biological Engineering and Computing*, July 1991, pp. 365-372.

11. J-Z. Wang, B. Tie, W. Welkowitz, J. L. Semmlow, and J. B. Kostis, "Modeling Sound Generation in Stenosed Coronary Arteries," *IEEE Transactions on Biomedical Engineering*, vol. 37, no. 11, November 1990, pp. 1087-1094.

12. Y. Ploysongsang, V. K. Iyer, and P. A. Ramamoorthy, "Inspiratory and Expiratory Vesicular Breath Sounds," *Respiration*, vol. 57, 1990, pp. 313-317.

13. A. C. Eycleshymer and D. M. Schoemaker, *A Cross-Sectional Anatomy*, Meredith Corporation, New York, 1970.

14. J. T. Dodge, G. Brown, E. L. Bolson, and H. T. Dodge, "Interthoracic Spatial Location of Specified Coronary Segments on the Normal Human Heart," *Circulation*, vol. 78, no. 5, November 1988, pp. 1167-1180.

15. R. T. Yen, Y. C. Fung, H. H. Ho, and G. Butterman, "Speed of Stress Wave Propagation in Lungs," *Journal of Applied Physiology*, vol. 61, 1986, pp. 701-705.

INITIAL DISTRIBUTION LIST

Addressee	No. of Copies
Defense Technical Information Center	12
Analysis & Technology (J. Kassal)	2
Medacoustics Corp. (A. Eberhardt, M. Nixon)	4
SCEEE Services Corp. (J. Foster)	2